MÖSSBAUER SPECTROSCOPY AND CRYSTAL CHEMISTRY OF AENIGMATITES

by

JIN BEOM CHOI

S.B. Seoul National University (1979)

M.S. Seoul National University (1981)

Submitted to the Department of
Earth and Planetary Sciences
in Partial Fulfillment of the
Requirements of the

Degree of

Master of Science

at the

MASSACHUSETTS INSTITUTE OF TECHNOLOGY

June, 1983

Signature of Author _____
Department of Earth and Planetary Sciences, March, 1983

Certified by _____
Thesis Advisor

Accepted by _____
Chairman, Department Committee

ABSTRACT

Aenigmatite, $Na_4^{VIII}(Fe^{2+},Ti,Fe^{3+})_{12}^{VI}(Si,Fe^{3+})_{12}^{IV}O_{40}$, is a common constituent of sodium-rich alkaline igneous rocks and is classified as an open-branched single-chain silicate, whose structure is closely related to that of sapphirine. The first Mossbauer spectra of three valid aenigmatite specimens were recorded and the detailed crystal chemistry were obtained. In the Mossbauer spectra, the extreme overlap of peaks for Fe^{2+} and Fe^{3+} cations in the low velocity region made fitting difficult and even made it impossible to resolve the liquid N_2 spectra. Moreover, the Mossbauer spectra are complicated by the possible occurrence of iron cations in seven octahedral and four tetrahedral sites. However, the Fe^{2+}-bearing octahedral sites were grouped into three categories, resulting in three quadrupole doublets. The Fe^{3+} cations in octahedral and tetrahedral sites were accounted for by three peaks. As a result, the stringent fitting of the room temperature spectra led to the resolution of nine peaks. Such peaks consist of three doublets of Fe^{2+}/oct and one combined peak at low velocity corresponding to two small peaks at high velocity which were assigned to Fe^{3+}/tet and Fe^{3+}/oct. Using the peak areas for Fe^{2+} and Fe^{3+} peaks, analytical data were reevaluated, including the comparison of Fe^{3+}/Fe^{2+} ratios determined by wet chemistry and by Mossbauer spectroscopy. As a result, electron microprobe

analyses were recalculated for FeO and Fe_2O_3 proportions and the crystal chemistry of aenigmatite was examined. Despite experimental errors involved, the existence of significant amounts of Fe^{3+} in tetrahedral coordination indicates that Fe^{3+} has a preference over Al^{3+} for the tetrahedral sites.

Thesis Supervisor: Roger G. Burns

Title: Professor of Mineralogy and Geochemistry

ACKNOWLEDGMENTS

The author wishes to express enormous thanks to his academic and thesis advisor, Professor Roger G. Burns who introduced him to the fantastic world of Mossbauer spectroscopy, encouraged him, gave valuable advice, and partly supported him throughout the research. Besides, Dr. Burns showed what the real scientist is and his enthusiasm for research. He always treated the author, who has been suffered from the unfamiliar American life, especially communications, kindly, friendly, generously, and much more.

The author is personally indebted to his parents for their support during his studies at M.I.T., and to his wife, Hye-Kyung who made it possible for him to complete this thesis successfully.

This thesis is dedicated to Roger who will stay in the author's mind as an example of a scientist as well as one of his best friends forever.

TABLE OF CONTENTS

LIST OF FIGURES AND TABLES

Page

LIST OF FIGURES

LIST OF TABLES

I. INTRODUCTION

1. What Is Aenigmatite?

Aenigmatite, discovered by Breighaupt in 1865, is commonly found in sodium-rich alkaline igneous rocks of both volcanic and plutonic parageneses (Merlino, 1970). It is classified as an open-branched single-chain silicate (Liebau, 1980). Because of its widely scattered occurrences, aenigmatite was described by numerous mineralogists after its discovery. However, uncertainties about its crystal chemistry and structure led to considerable confusion in the earlier literature, until the intensive study by Kelsey and McKie (1964) clarified structural and chemical properties of aenigmatite.

Although the origin of its name is not clear, one of the aenigmas of the mineral aenigmatite is that it has been called many different names as a result of earlier uncertainty regarding its composition. Cossyrite, derived from the pantellerite lavas of Pantelleria the ancient name for which was Cossyra (Föstner, 1881), was considered to be the same mineral, but now the name is rarely used. Köbingite, considered as a pseudomorph of aenigmatite by its discoverer (Breithaupt, 1865), was discredited as an arfvedsonite-aenigmatite intergrowth (Brögger, 1890). This confusion over name and identity still exists: two specimens made available to us from the Harvard collection (85123 & 85123A) turned out to be an arfvedsonite,

and the mineral called aenigmatite in a recent paper (Steffen and Seifer, in press) appears to be riebeckite-arfvedsonite rather than aenigmatite.

2. Crystal Structure

The crystal morphology of aenigmatite, studied imperfectly by early workers, was determined to be triclinic with unit-cell constants: a : b : c = 1.0050 : 1 : 0.5862, $\alpha = 96°59.5'$, $\beta = 96°49.5'$, $\gamma = 112°28'$ (Palache, 1933). The first detailed X-ray study was done by Kelsey and McKie (1964) using a crystal of aenigmatite from the Kola peninsula, U.S.S.R. (AEN1, Cambridge 38075)*. Unit-cell parameters are shown in Table 1. They reported chemical analyses of twelve specimens from eight different localities and characterized the chemical unit of aenigmatite as the idealized formula $Na_4Fe^{2+}_{10}Ti_2Si_{12}O_{40}$. They suggested the crystal structure of aenigmatite contains silicate chains of pyroxene type cross-linked by Ti^{4+} and Fe^{2+} on distinct octahedral sites with Na on sites of higher coordination number. However, the complete structure remained unsolved until two independent and simultaneous determinations were reported by Merlino (1970) and Cannillo, et al. (1971) who collected X-ray data from aenigmatite crystals from Naujakasik, Greenland (AEN3, Harvard 85124)*.

* Numbers refer to specimens described in Table 2.

According to Merlino (1970) and Cannillo, et al. (1971), the crystal structure of aenigmatite is closely related to that of sapphirine. In fact, the crystal structure of aenigmatite could be deduced from the structure of sapphirine (Moore, 1969; Merlino, 1973, 1980). In spite of their different chemical compositions, there are significant crystallochemical similarities between aenigmatite and sapphirine. As shown in Table 1, unit-cell parameters of sapphirine are analogous to those of aenigmatite. Moreover, the triclinic cell can be described in terms of a multiple (four-fold) pseudomonoclinic cell obtained by applying the transforming matrix of

Table 1. Unit cell parameters of aenigmatite and sapphirine

	Aenigmatite		Sapphirine	
	Cannillo et al. (1971)	Kelsey and McKie (1964)	Merlino (1973)	
	pseudo-monoclinic	triclinic	pseudo-monoclinic	triclinic
a Å	12.120	10.406	11.33	10.04
b Å	29.63	10.813	29.08	10.38
c Å	10.406	8.926	10.04	8.65
α	90°04'	104°56'	90°	107°33'
β	127°9'	96°52'	125°23'	95°07'
γ	89°44'	125°19'	90°	123°55'
Z	8	2	8	2

[100/$\bar{1}$22/100] to the triclinic cell. Cannillo, et al. (1971) suggested that the ideal chemical formula of aenigmatite is $Na_2^{VIII}(Fe^{2+},Ti,Fe^{3+})_6^{VI}O_2[(Si,Fe^{3+})_6^{IV}O_{18}]$.

In sapphirine, $(Mg,Fe,Al)_8^{VI}O_2[(Si,Al)_6^{IV}O_{18}]$, "walls" of $(Mg,Fe,Al)O_6$ octahedra run infinitely along the z axis parallel to (100) and are separated from each other in the y direction. The walls are interconnected by chains of tetrahedra running along (001) as well as by additional Al octahedra (Moore, 1969). In aenigmatite, however, some modifications to the sapphirine structure occur because some octahedra are replaced by Na-polyhedra of higher coordination, that is, distorted square antiprisms. The octahedral walls, therefore, are build up of continuous (100) layers formed by both (Fe,Ti) octahedra and Na-antiprisms (Fig. 1a) instead of bands in sapphirine. Tetrahedra chains are, as in sapphirine, pyroxene-like single chains, with additional "wings" of corner-sharing tetrahedra, though the chains are somewhat less kinked in aenigmatite than in sapphirine (Fig. 1b). Oxygens in sapphirine are in cubic close-packed array, whereas those in aenigmatite are too puckered to approximate close-packing.

In aenigmatite, there are six crystallographically independent tetrahedral sites which can be divided into two groups: 1)tetrahedra [T(1) and T(4)] having one non-bridging oxygen, and 2) tetrahedra [T(2), T(3), T(5), and T(6)] having two non-bridging oxygens; however, the difference of Si-O

Fig. 1. Idealized polyhedral diagrams of aenigmatite: a) layer of (Fe,Ti) octahedra and Na-antiprisms lying in the (100) plane, parallel to z axis (pseudomonoclinic cell), b) layer of tetrahedral $[Si_6O_{18}]_\infty$ chains connected by single octahedra. ∘ shown in two different layers represent same positions. From Cannillo, et al. (1971)

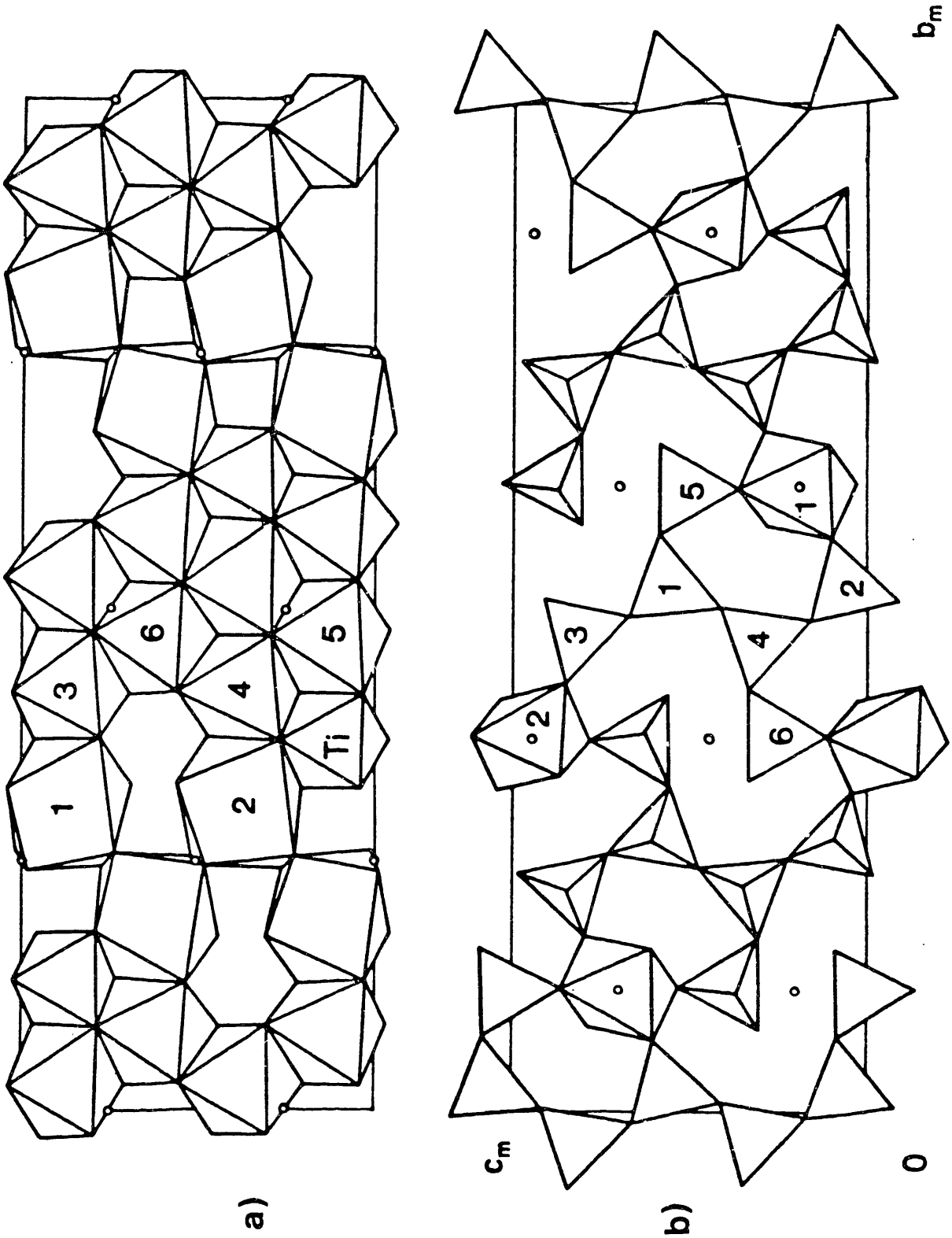
a)
1
2
3
4
5
6
Ti
b)
b_m
c_m
0
1
2
3
4
5
6
1°
2°

distances between the two groups is not significant and the range of distances is 1.59 to 1.69 Å (Cannillo, et al., 1971). It is difficult to determine where ferric ions occur in the six tetrahedral sites but the small amount of Fe^{3+} available for distribution was assumed to preferentially occupy the T(3) site (Cannillo, et al., 1971).

Seven different octahedral sites exist in aenigmatite. All have almost the same range of metal-oxygen distances, 2.10 to 2.17 Å, except the octahedron around M(7) which is believed to be preferentially occupied by Ti^{4+} and has a range of distances of 1.84 to 2.09 Å (average 1.98 Å). This M(7) site is also believed to be occupied by some Fe^{3+} and perhaps Fe^{2+} cations. The other six M sites are occupied mainly by Fe^{2+} cations and minor amounts of Ca^{2+}, Mn^{2+}, Mg^{2+}, and Fe^{3+} cations. The M sites except M(7) can be divided into three different groups in terms of types of bridging oxygens. They are 1) M(5) with two non-bridging oxygens, 2) M(3), M(4), and M(6) having one non-bridging oxygen and "neutral" electrostatic balance, and 3) M(1) and M(2) having similar non-bridging oxygen as in the second group, but with "underbonded" oxygens. This forms the basis for the fitting of the Mossbauer spectra of aenigmatite described in Chap. II.

Minerals being isostructural with aenigmatite include rhönite, $Ca_4(Mg,Fe^{2+})_8Fe_2^{3+}Ti_2(Al_6Si_6O_{40})$, which has the same sapphirine-like monoclinic pseudo-cell (Cameron, et al., 1970);

krinovite $Na_2Mg_2CrSi_3O_{10}$ (Merlino, 1972); and serendibite $Ca_2(Mg,Al)_6O_2[(Si,Al,B)_6O_{18}]$ (Machin & Süsse, 1974). Merlino (1972) suggested that Cr in the krinovite structure occupies the M(1), M(2) and M(8) sites, and Mg occurs in the remaining octahedra.

3. Parageneses

Aenigmatite is a common consituent of sodium-rich alkaline igneous rocks. In volcanic parageneses, such as the pantellerites, pantelleritic trachytes, and comendites of Pantelleria and Kenya Rift Velley, the alkali lavas of Oki Island, Japan, and the comendites of Mt. Nimrud, Armenia, etc., aenigmatite occurs as a component of the groundmass, and less frequently as a phenocryst. Chemical analyses indicate that aenigmatite-bearing rocks are characterized by rather high titanium contents and relatively low iron oxidation ratio (Kelsey and McKie, 1964).

Aenigmatite is commonly associated with anorthoclase, aegirine-hedenbergite and quartz in Pantelleria lavas and titanomagnetite in peralkaline trachytes in New South Wales, Australia. Zoned aenigmatite with cores of titanomagnetite indicates titanomagnetite reacts with sodium silicate liquid, and then aenigmatite crystallizes at low oxygen fugacity. The reaction may be represented as follows:

$$6\ (TiFeO_3 \cdot Fe_3O_4) + 12\ SiO_2 + 12\ (NaFe^{3+}Si_2O_6 + CaFe^{2+}Si_2O_6)$$
titanomagnetite — aegirine - hedenbergite

$$\leftrightarrow\ 6\ (Na_2Fe_5^{2+}TiSi_6O_{20}) + 12\ CaFe^{2+}Si_2O_6 + 2\ Fe_3O_4 + 5\ O_2 \uparrow$$
aenigmatite — hedenbergite — magnetite

This kind of reaction may explain why analytical data of most aenigmatites show low Fe^{3+}/Fe^{2+} ratios. The temperature and oxygen fugacity operating during the formation of the aenigmatite is estimated to be 900 ± 50 °C and $10^{-12.60}$ to $10^{-13.7}$ atm, respectively (Deer, et al., 1978).

Another paragenesis of aenigmatite is plutonic and includes nepheline and sodalite-syenites of Kangerdluarsuk, west Greenland; a micro-syenite vein from South Boswell Bay, east Greenland (AEN2, Deer 3584)*; the foyaite and khibinite pegmatites in Kola peninsula (AEN1, Cambridge 38075)*; monzonites and syenites from the Morotu River, Japan; and aegirine-syenites in Madagascar, etc. In these occurrences, aenigmatite is commonly associated with aegirine, riebeckite and hastingsite. Aenigmatite is sometimes replaced by albite and riebeckite during later periods of albitization. Astrophyllite and, less commonly, biotite also replace aenigmatite.

Aenigmatite also occurs in more silicic plutonic rocks, such as nordmarkite of Maine and granite-complexes of Nigeria, where aenigmatite is usually associated with aegirine and arfvedsonite-riebeckite.

---

* Numbers refer to specimens described in Table 2.

4. Purpose and Method of Study

Although aenigmatite is easily recognized in common igneous rocks and has received some attention from mineralogists, its detailed crystal chemistry is poorly understood and was even misinterpreted in a recent study (Steffen & Seifer, in press). The determination of cation site occupancies is not easy because there are several different crystallographic positions in the aenigmatite structure. Moreover, iron ordering over tetrahedral and/or octahedral sites is also controvertial.

In this work, the author set out to determine the distribution of Fe^{2+} and Fe^{3+} over different cation sites by measuring the Mossbauer spectra of several aenigmatites. In order to accomplish this goal, certain conditions had to be met. First, proper specimens of natural aenigmatite were carefully collected. In this step, all specimens were identified by the X-ray diffraction because some amphiboles could be misidentified as aenigmatite. Second, Mossbauer measurements were made on specimens having different compositions at both room temperature and liquid N_2 temperature (80°K). Consistencies in peak positions as well as parameters among different specimens were established to demonstrate the accuracy of fitting which should be important for first Mossbauer works about aenigmatite. Third, distribution of iron cations over the octahedral and tetrahderal sites were determined from the Mossbauer parameters,

and the crystal chemistry of aenigmatite was finally obtained.

X-ray diffraction analyses were made by a DIANO digital model X-ray diffractometer using Fe-filtered Co radiation (30KV/15mA), available in the X-ray Diffraction Laboratory in the Department of Material Sciences, M.I.T. Mossbauer spectra were recorded on a constant acceleration ASA (Austin Science Associates) Mossbauer spectrometer, using 512 channels of a 1024 channel Nuclear Data multichannel analyser. The spectra were acquired from two different ends of a vibrator designed for dual purpose; one end of the vibrator having a ^{57}Co source in a rhodium matrix (90-100 milicuries) was used for liquid nitrogen spectra, and the other end having a ^{57}Co source in a palladium matrix (40-50 milicuries) was used for room temperature measurements. Sample preparation and fitting procedures will be discussed in Chap. II.

II. EXPERIMENTAL PROCEDURES

1. Aenigmatite Specimens

Eight aenigmatite specimens with different parageneses were collected for this study. Three of the samples came from Cambridge University and were the very specimens used in the study by Kelsey and McKie (1964). The remaining aenigmatites were obtained from the mineralogical collection at Harvard University. However, two of them (Harvard 85123 & 85123A) were disquailified as being arfvedsonites and were discarded from this study.

After a preliminary examination of the Mossbauer spectra of all the aenigmatites, three typical specimens were selected for detailed Mossbauer experiments and computer fitting. Localities of specimens chosen in this study are listed in Table 2 and chemical analyses are shown in Table 3.

Table 2. Localities of aenigmatite specimens.

AEN1	aenigmatite from Khibinite quarry, east of Kirovsk, Kola, USSR. Obtained in powder form from Cambridge Univ., #38075.
AEN2	aenigmatite from South Boswell Bay, Kangerdlugsuak, East Greenland. Obtained in powder form from Cambridge Univ., Specimen W. A. Deer #3584.
AEN3	aenigmatite from Naujakasik, Greenland. Obtained in the form of a hand specimen from Harvard University #85124.

2. Mossbauer Spectra

Sufficient aenigmatite samples were weighed out so as to give a total iron concentration of approximately 7.5 mg/cm^2. A recent study (M.D. Dyar, pers. comm., 1982) confirmed that the optimum range of total iron concentrations for most Fe-bearing silicates is 5-10 mgFe/cm^2 to get a relatively good absorbance in the Mossbauer spectra and best statistics. The weighed sample was mixed with sugar, ground under acetone (which helps to prevent ferrous iron from oxidation), mounted in a round hole of 2.2 cm diameter sealed by cellotape in a plastic square plate, and shielded by a lead square plate with

Table 3. Uncorrected chemical analyses of aenigmatite specimens.

	AEN1[a]	AEN2[b]	AEN3[c]
SiO_2	39.62	41.41	40.24
TiO_2	9.66	8.30	7.52
Al_2O_3	0.64	nil	1.31
Fe_2O_3	4.64	4.46	} 41.13**
FeO	33.92	35.87	
MnO	2.46	1.78	0.83
MgO	1.65	1.35	0.01
CaO	0.44	nil	0.13
ZnO	*	*	0.17
Na_2O	7.20	6.87	7.75
K_2O	0.04	0.04	0.06
H_2O^+	0.05	nil	*
H_2O^-	nil	n.d.	*
Cl	0.02	n.d.	*
F	nil	n.d.	*
Σ	100.34	100.08	99.15

a: wet analysis by J.H. Scoon (S.O. Agrell, pers. comm., 1982)
b: wet analysis by P.E. Brown & Mrs. Chadwick (S.O. Agrell, pers. comm., 1982)
c: microprobe analysis by D.A. Nolet (R.G. Burns, pers. comm., 1982)
*: element not analyzed
**: determined as FeO

the same diameter hole. For low temperature runs, the plastic disc containing the sample was attached to a copper rod suspended in a reservoir of liquid nitrogen (80°K). The spectra were run for 1-2 days to acquire more than 10^6 counts per channel within the velocity range of ± 5 mm/sec.

The Mossbauer spectra were calibrated relative to Fe foil and transferred to a MINC PDP 11/23 minicomputer, where the plotting and the calculations for curve-fitting were executed. Examples of unfitted Mossbauer spectra of specimen AEN1 at both 300°K (room temperature) and at 80°K (liquid N_2 temperature) are shown in Fig. 2a and 2b.

As illustrated in Fig. 2, the spectra show two characteristic regions dominated by absorption by Fe^{2+} components at approximately zero and 2.3 mm/sec in the room temperature spectrum; the high velocity peak increases by about 0.3 mm/sec in the liquid N_2 spectrum. Comparing the area of two peaks, the low velocity region has higher absorption than the high velocity one, resulting from overlap of Fe^{2+} and the low velocity Fe^{3+} components. The very small, broad peak at approximately 0.9 mm/sec represents absorption by the high velocity peak of Fe^{3+} components; the peak is better resolved in the liquid N_2 temperature spectrum. The strong overlap of Fe^{2+} and Fe^{3+} peaks in the low velocity region and the small intensities of the Fe^{3+} components require very stringent constraints in the fitting procedures. Mossbauer spectra of

Fig. 2. Unfit Mossbauer spectra of aenigmatite AEN1. A) 300°K spectrum (room temperature); B) 80°K spectrum (liquid N_2). The spectra show two regions dominated by absorption by Fe^{2+} ions at approximately zero and 2.5 mm/sec. The small peak at approximately 0.9 mm/sec originates from Fe^{3+} ions.

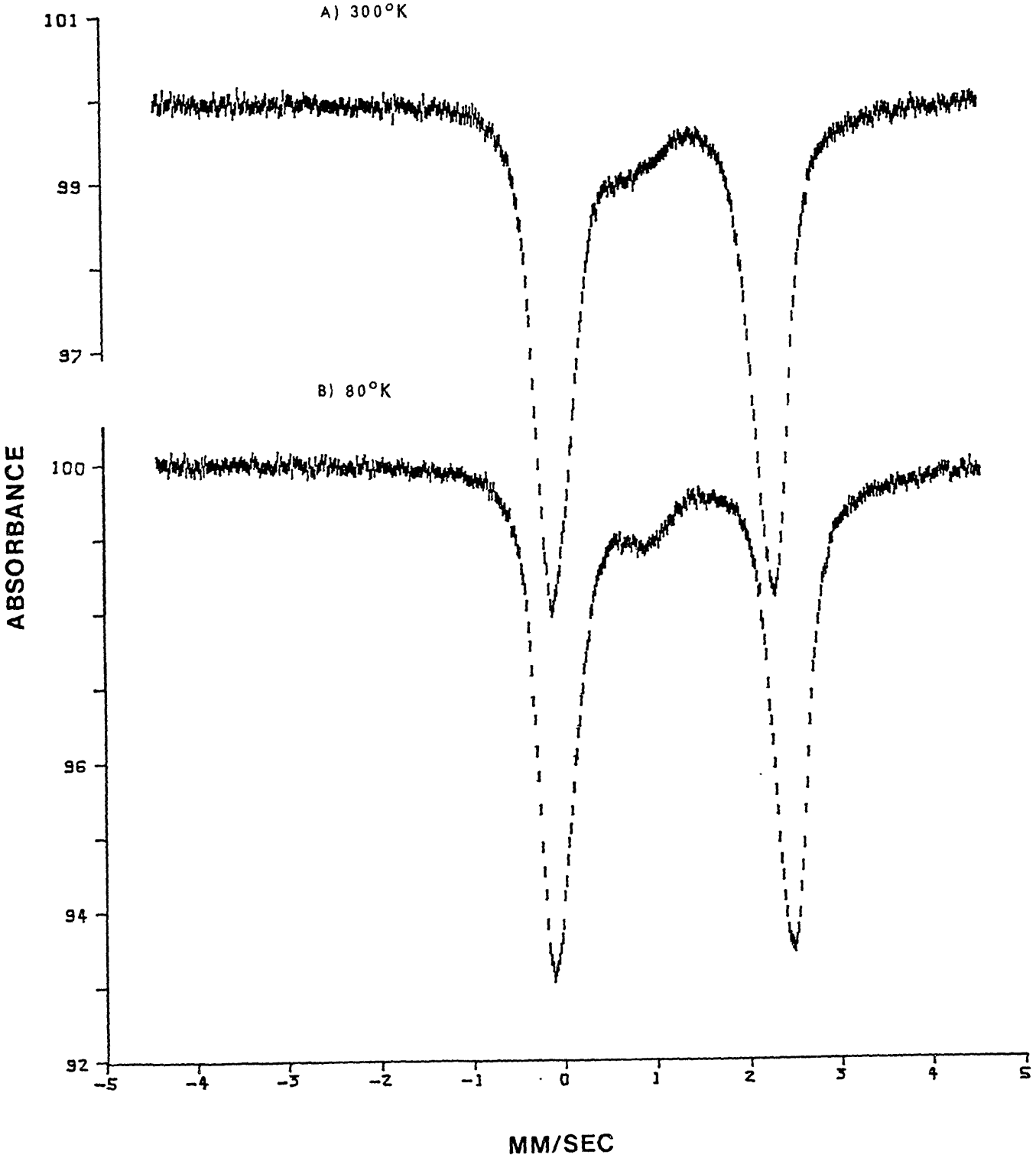
A) 300°K
B) 80°K
101
99
97
100
96
94
92
ABSORBANCE
-5
-4
-3
-2
-1
0
1
2
3
4
5
MM/SEC

other aenigmatie specimens are similar to that of AEN1 shown in Fig. 2.

3. Fitting Procedures

The Mossbauer spectra were fitted with a least-squares program, developed by A. J. Stone (Stone, et al., 1969), modified by Huggins (1974), and adapted for the PDP11/23 computer by Dr. K. M. Parkin and M. D. Dyar. Stone's program fits a sum of Lorenzian curves using the Gauss non-linear regression method with appropriated constraints on the various input parameters.

Prior to attempts to fit the aenigmatite spectra, it was necessary to assess the number and type of cation sites for Fe^{2+} and Fe^{3+} in the structure of aenigmatite. As already discussed in Chap. II, there are seven different octahedral sites, including the M(7) site assigned to Ti^{4+}, and four different tetrahedral sites in aenigmatite. However, the resolution of peaks to individual iron cations in each of these sites is impossible, so that it was necessary to group the sites into distinguishable groups. As noted earlier, the assumption was made that grouping of six M sites into three categories could be made: [M(1) & M(2)], M(5), and [M(3), M(4) & M(6)] leading to the resolution of three Fe^{2+} doublets. Although ferric iron is assumed to occupy the tetrahedral T(3) site preferentially (Cannillo, et al., 1971), the breadth of

the inner peak suggests the existence of two Fe^{3+} doublets. While one doublet may originate from Fe^{3+} cations in the T(3) site, the other doublet may represented ferric ions in another tetrahedral site, or possibly ferric ions in octahedral sites.

Another factor to be considered in the peak assignments is whether the aenigmatite spectra show evidence for mixed-valence iron cation species. Burns (1981) suggested that silicates with infinite chains of edge-shared Fe^{2+}-Fe^{3+} octahedra such as ilvaite, vivianite, deerite, and glaucophane-riebeckite, etc. permit electron delocalization between Fe^{2+} and Fe^{3+} which leads to a mixed-valence state of $Fe^{2.5+}$. He also classified aenigmatite as one of the mixed-valence silicate minerals that had the potential for exhibiting electron delocalization. The phenomenon of mixed-valence iron cation species is very well detected by the Mossbauer effect because the isomer shift parameter is intermediate between values for discrete Fe^{2+} and Fe^{3+} cations (McCammon & Burns, 1980; Nolet & Burns, 1979).

Due to the extreme overlap in the low velocity region and relatively small intensities of ferric peaks, initial attempts to fit aenigmatite spectra started with six peaks consisting of two ferrous doublets and two ferric peaks at high velocity in order to determine the ferric peak positions. Then two more peaks were added in the low velocity region to match the ferric peaks at high velocity but the fits diverged due to

severe overlap of Fe^{2+} and Fe^{3+} peaks in the low velocity region. In order to solve these problems, combining of the two small ferric peaks at low velocity was introduced which led to convergence, but the area of the combined peak did not correspond to the sum of two independent high velocity Fe^{3+} peak areas. Next, additional constraints fixing peak positions as well as constraining area values were applied to the combined low velocity Fe^{3+} peak such that its area equalled the sum of two small ferric peaks at high velocity. This led to convergence with a chi-square value of 750 ± 50. Finally, a third Fe^{2+} doublet was added in accord with the assumption of grouping Fe^{2+} sites into three distinguishable categories. Then, convergence was achieved and the χ^2 was lowered to a more reasonable value of 550 ± 50.

To illustrate the fitting procedures, the results of the spectrum of AEN2 fitted to seven and nine peaks are shown in Fig. 3 and Fig. 4, respectively, and their parameters are summarized in Table 4. Table 4 shows that there are insignificant variations of isomer shift (δ), quadrupole splitting (Δ), and Fe^{3+} peak areas between the two fitted spectra, while the χ^2 value is decreased significantly from 760 in the seven-peak fit to 552 in the nine-peak fit. However, releasing constraints and permitting individual doublets to attain separate width values made convergence difficult and produced very broad and anomalous widths of ferric peaks

Table 4. Mossbauer parameters from two different fitting schemes for AEN2

	doublet**	δ*	Δ*	Width*	%Area	χ^2
Seven peaks						
Fe2+(I)	1-2	1.119	2.538	0.342	60.95	
Fe2+(II)	3-4	1.116	2.214	0.342	28.47	
Fe3+/tet	5-6	0.276	0.643	0.342	5.83	760
Fe3+/oct	5-7	0.488	1.068	0.342	4.64	
Nine peaks						
Fe2+(I)	1-2	1.116	2.586	0.319	47.92	
Fe2+(II)	3-4	1.136	2.311	0.319	25.03	
Fe2+(III)	5-6	1.175	2.025	0.319	16.35	593
Fe3+/tet	7-8	0.281	0.652	0.319	5.88	
Fe3+/oct	7-9	0.490	1.071	0.319	4.82	

* all values in mm/sec relative to Fe foil

** numbers refer to Fig. 3 and Fig. 4.

Fig. 3. The spectrum of AEN2 at room temperature fitted with seven peaks. The doublets 1-2, 3-4 are dominated by Fe^{2+} components and the doublets 5-6, 5-7 by Fe^{3+} components.

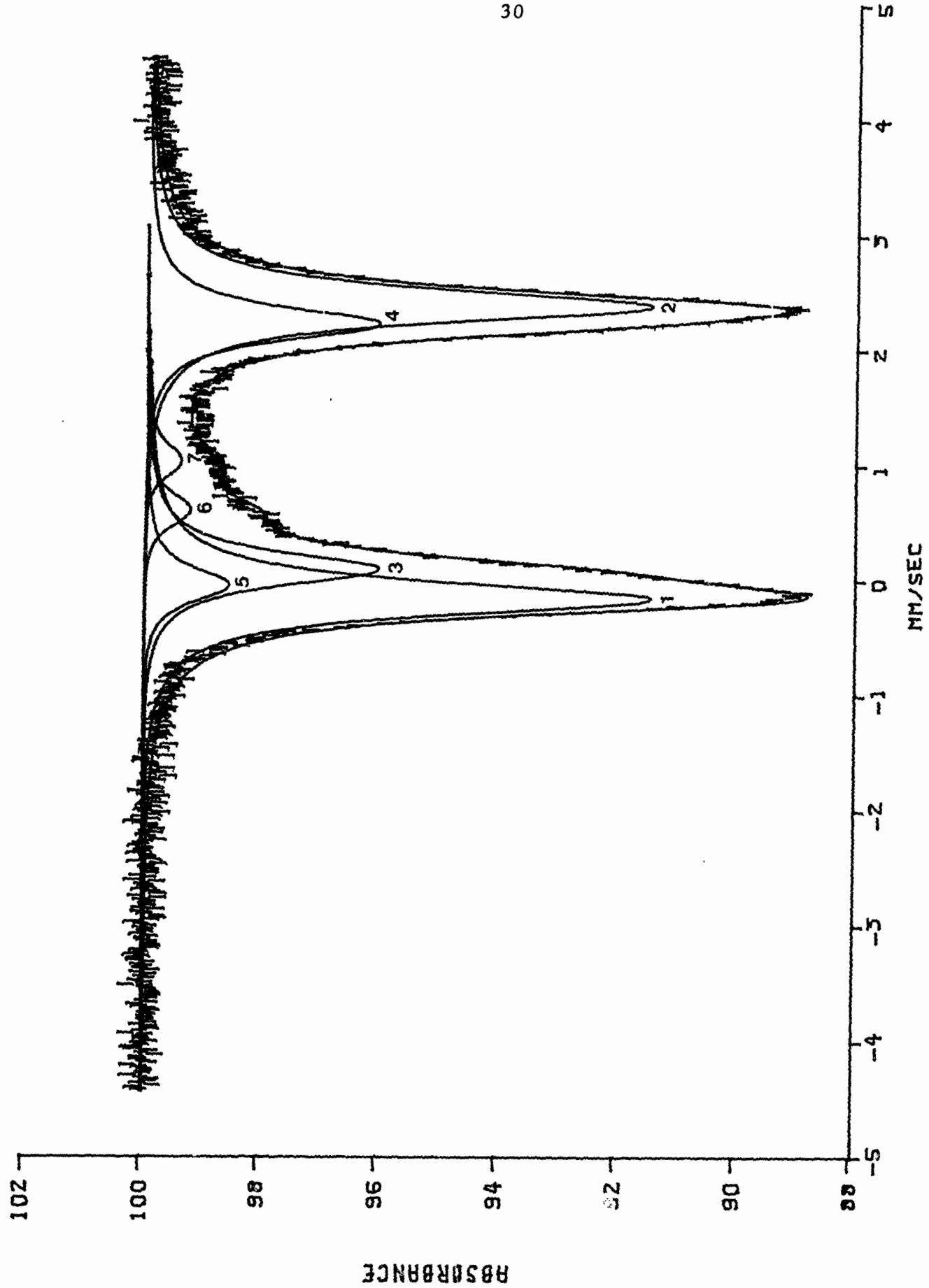
ABSORBANCE
102
100
98
96
94
92
90
88
-5
-4
-3
-2
-1
0
1
2
3
4
5
MM/SEC
1
2
3
4
5
6
7

Fig. 4. The spectrum of AEN2 at room temperature fitted with 9 peaks. The doublets 1-2, 3-4, 5-6 are dominated by Fe^{2+} components and the doublets 7-8, 7-9 by Fe^{3+} components.

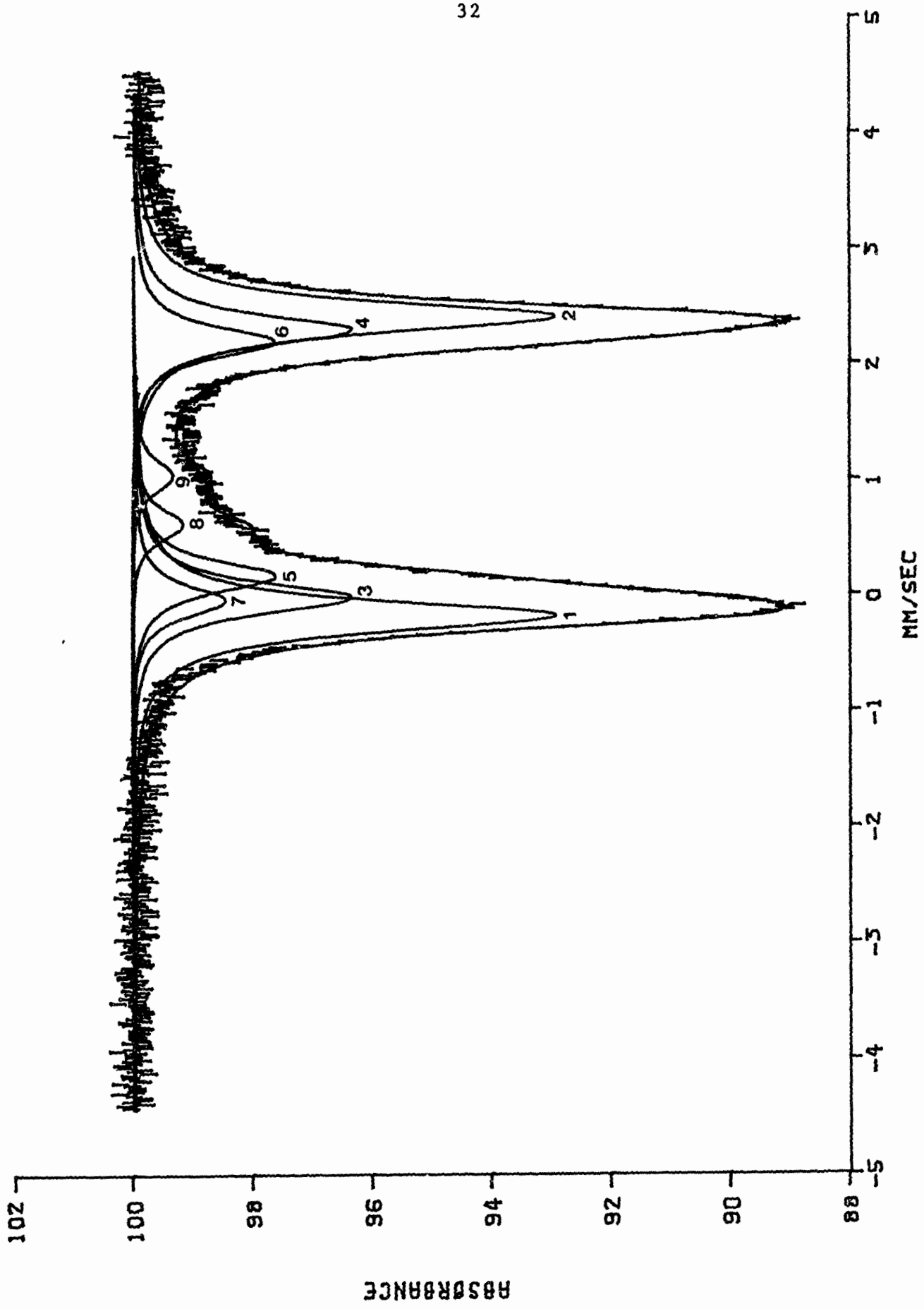
ABSORBANCE
102
100
98
96
94
92
90
88
-5
-4
-3
-2
-1
0
1
2
3
4
5
MM/SEC
1
2
3
4
5
6
7
8
9

despite the slight decrease of the χ^2 in both fitting steps.

The resolution of more than three ferrous doublets or the resolution of two independent ferric doublets, even with heavy constraints (that is, fixed position and fixed areas), were unsuccessful so that the nine-peak fitting scheme was adopted as the final procedure for the other aenigmatite spectra.

Attempts to fit the liquid N_2 spectra were unsuccessful and positions of ferric peaks in the low velocity region could not even be found. No convincing explanation can be given for the divergence. However, one possible reason is that while there is a small increase in isomer shift with decreasing temperature for both Fe^{2+} and Fe^{3+}, the variation of quadrupole splitting is significant for Fe^{2+} (usually 0.2 - 0.5 mm/sec) but is negligible for Fe^{3+} (0 - 0.03 mm.sec). This phenomenon usually aids the resolution of closely overlapping peaks in the low velocity region in most Mossbauer spectra. In the case of the aenigmatite spectra, however, the strong overlap of Fe^{2+} and Fe^{3+} in the low velocity region makes the resolution more difficult with decreasing temperature. In other words, with decreasing temperature the positions of ferrous peaks at low velocity move outward to lower velocity, which makes the second and the third ferrous peaks more closely overlap the ferric

Table 5. Peak positions for Mossbauer spectra of aenigmatite specimens at room temperature.

	Fe^{2+} (I)	Fe^{2+} (II)	Fe^{2+} (III)	Fe^{3+} /tet	Fe^{3+} /oct
AEN1	-0.17	0.01	0.19	-0.05	0.05
	2.35	2.21	2.08	0.71	1.02
AEN2	-0.18	-0.02	0.16	-0.05	-0.05
	2.41	2.29	2.19	0.61	1.02
AEN3	-0.15	0.05	0.22	-0.03	-0.03
	2.36	2.22	2.15	0.63	1.04

All values in mm/sec are relative to Fe foil

Fig. 5. Peak Positions for Mossbauer spectra at room temperature. Note the consistency of peak positions among the different specimens. (Numbers represent different Fe^{2+} groups and T and O represent tetrahedral and octahedral Fe^{3+} components, respectively.)

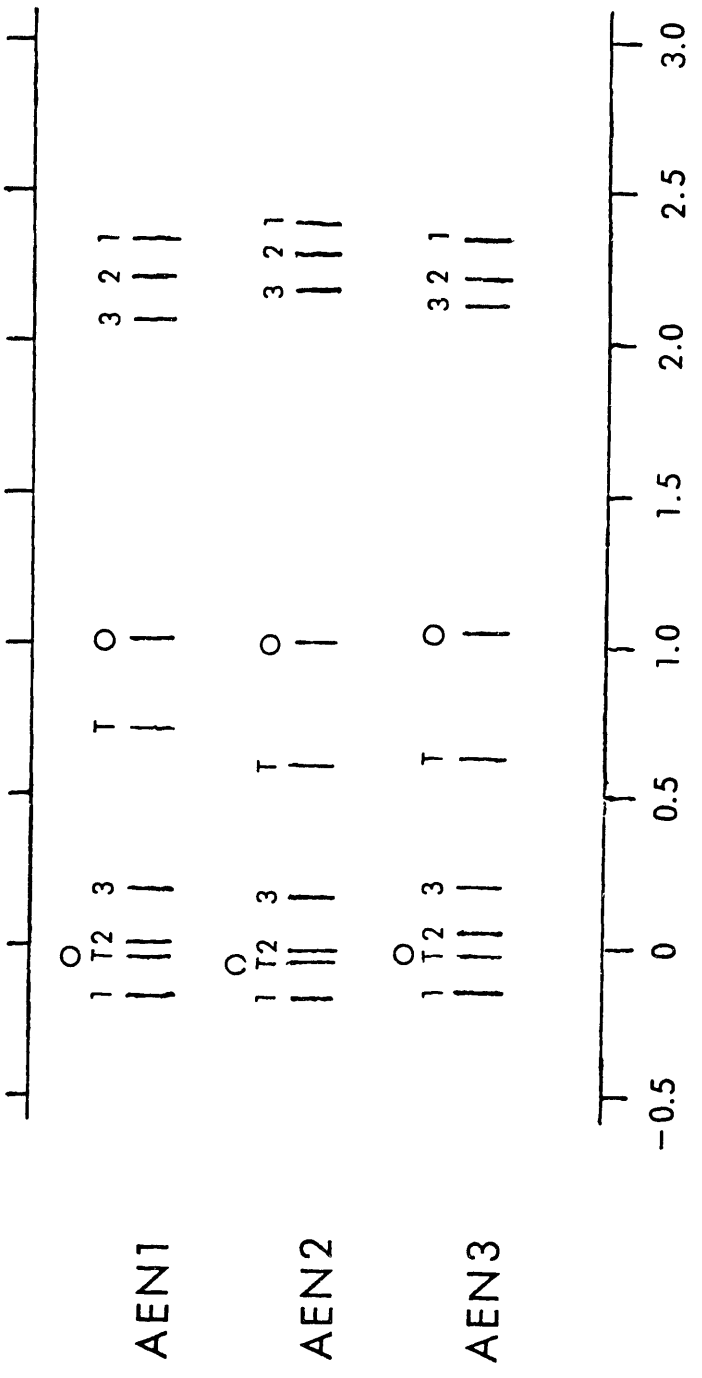
AEN1
AEN2
AEN3
O
1 T2 3
T
O
3 2 1
−0.5
0
0.5
1.0
1.5
2.0
2.5
3.0
MM/SEC

Fig. 6. The fitted spectrum of AEN1 at room temperature. (Numbers refer to Fig. 4.)

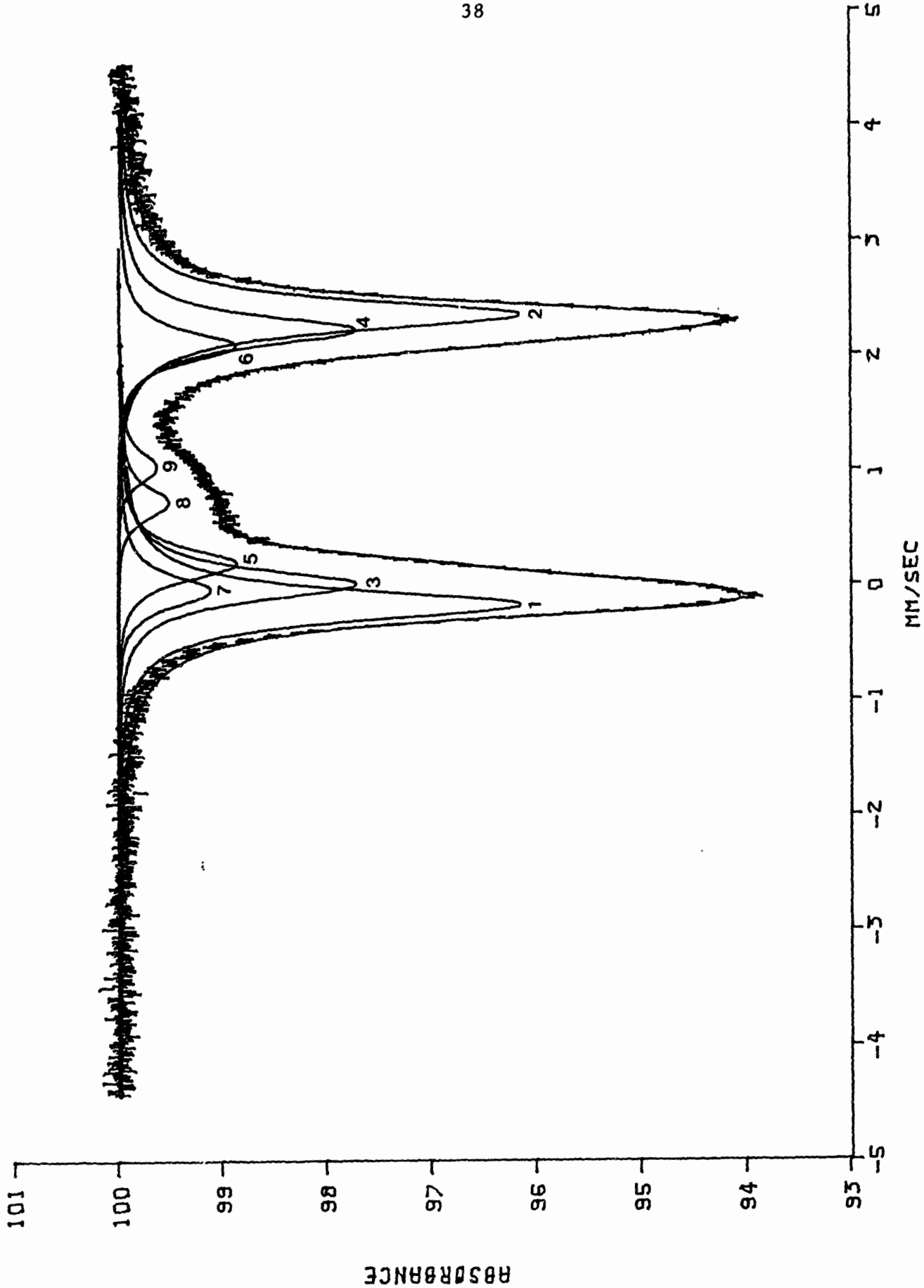
ABSORBANCE
101
100
99
98
97
96
95
94
93
-5
-4
-3
-2
-1
0
1
2
3
4
5
MM/SEC
1
2
3
4
5
6
7
8
9

Fig. 7. The fitted spectrum of AEN3 at room temperature. (Numbers refer to Fig. 4.)

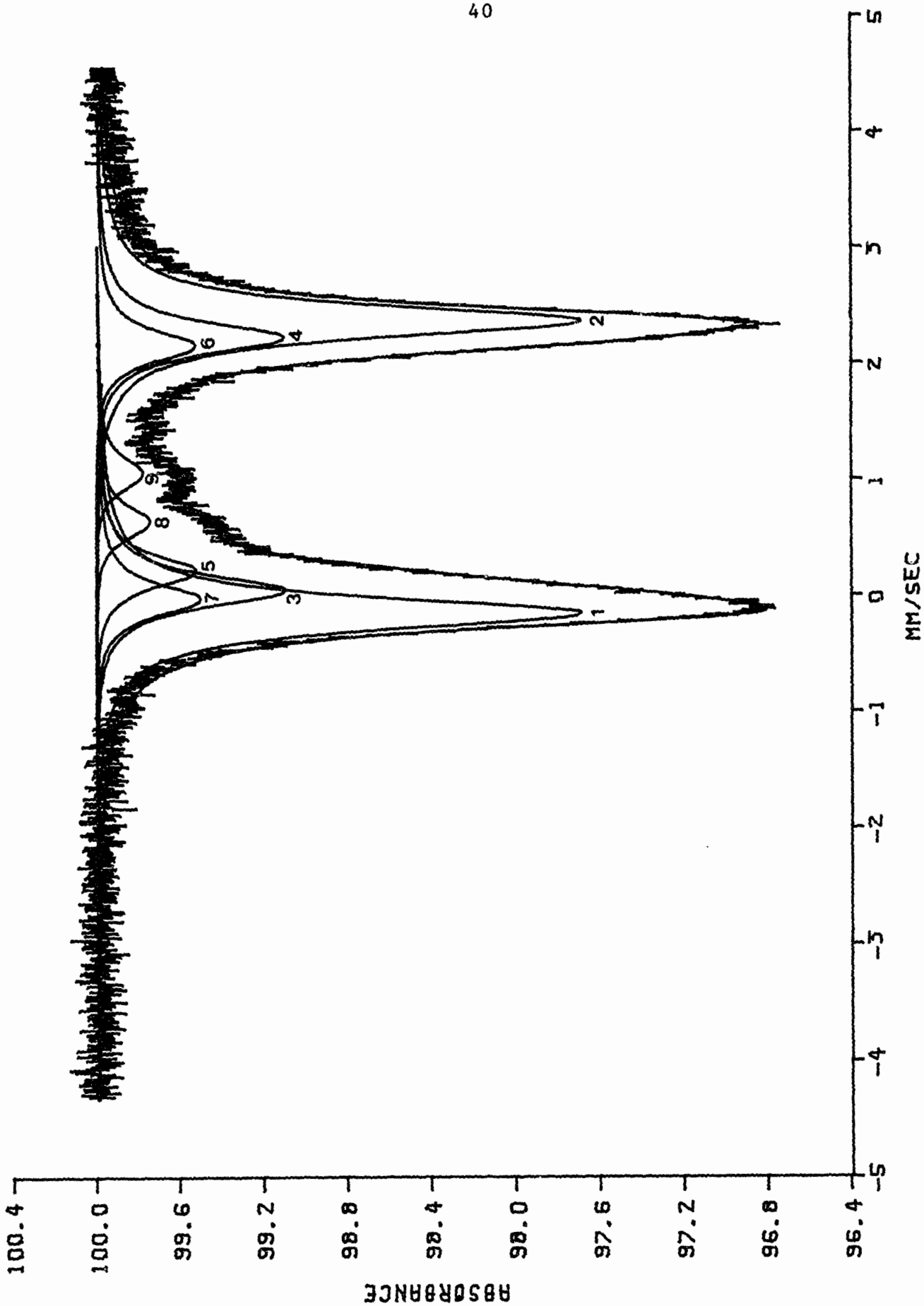
100.4
100.0
99.6
99.2
98.8
98.4
98.0
97.6
97.2
96.8
96.4
ABSORBANCE
-5
-4
-3
-2
-1
0
1
2
3
4
5
MM/SEC
1
2
3
4
5
6
7
8
9

Table 6. Mossbauer parameters of AEN1 and AEN3** at room temperature.

	doublet	δ*	Δ*	Width*	%Area	χ^2
AEN1						
Fe^{2+}(I)	1-2	1.087	2.520	0.319	46.86	
Fe^{2+}(II)	3-4	1.111	2.206	0.319	27.93	
Fe^{2+}(III)	5-6	1.132	1.887	0.319	14.62	563
Fe^{3+}/tet	7-8	0.334	0.760	0.319	6.24	
Fe^{3+}/oct	7-9	0.488	1.066	0.319	4.83	
AEN3						
Fe^{2+}(I)	1-2	1.106	2.512	0.328	54.86	
Fe^{2+}(II)	3-4	1.134	2.169	0.328	21.52	
Fe^{2+}(III)	5-6	1.181	1.930	0.328	11.56	565
Fe^{3+}/tet	7-8	0.302	0.658	0.328	6.44	
Fe^{3+}/oct	7-9	0.510	1.074	0.328	5.63	

* all values in mm/sec relative to Fe foil

** AEN2 are listed in Table 4.

combined peak. This resulted in the failure of finding the peak positions for these three components in the liquid N_2 temperature spectra.

Having now obtained the number of peaks (actually nine), peak positions, and widths, two other room temperature spectra of aenigmatites AEN1 and AEN3 were fitted with similar constraints to those for AEN2. The results of both the seven- and nine-peak fits converged and are in good agreement with those of AEN2. Table 5 and Fig. 5 show that the consistencies of the peak positions among different spectra are well established, which is one of the main criteria sought in this study. The fitted apectra of AEN1 and AEN3 are shown in Fig. 6 and Fig. 7, respectively and their parameters are summarized in Table 6.

III. RESULTS

1. Mossbauer Parameters

According to the procedure discussed in Chapter II, all final spectra were fitted with nine peaks, that is, three doublets and a combination peak corresponding to two independent ones. Their Mossbauer parameters are summarized in Table 4 and Table 6.

The isomer shifts (δ) obtained for Fe^{2+} in aenigmatite are in the range 1.106 - 1.181 mm/sec except for the slightly lower value of 1.087 mm/sec for the doublet 1-2 of AEN1. These values agree well with the isomer shifts for Fe^{2+} in octahedral sites in other silicates. The area ratios for the three ferrous doublets I : II : III are roughly 3 : 2 : 1, which correlates with the multiplicity of sites in terms of the grouping of the six octahedral sites in aenigmatite. Therefore, the assignment for the Fe^{2+} doublets is that Fe^{2+}(I) is attributed to the absorption by the sites M(3), M(4) and M(6), Fe^{2+}(II) by the sites M(1) and M(2), and Fe^{2+}(III) by the M(5) site, respectively.

In the assignment of the Fe^{3+} peaks, the Mossbauer parameters suggest different site occupancies from those deduced from published chemical analyses done by Kelsey and McKie (1964). The isomer shifts of Fe^{3+} are divided into two types;

one type has large values of 0.488 - 0.510 mm/sec which are consistent with ferric iron in octahedral coordination. The other type has the smaller values of 0.28 - 0.33 mm/sec corresponding to isomer shifts for tetrahedrally coordinated ferric ions. Actually, the isomer shifts for most compounds with Fe^{3+} in tetrahedral coordination fall into the range of 0.2 to 0.3 mm/sec. The isomer shift is a function of the s-electron density at the nucleus, as compared with their density at the source nucleus. For iron cations, the isomer shift increases with decreasing s-electron density. The isomer shifts of ferric ions in tetrahedral environments are strongly dependent on the average metal-oxygen distances which affect the s-electron density at the nucleus of ferric iron, that is, increasing in average metal-oxygen distances by substituting bigger cation decreases in s-electron density at nucleus. Thus, isomer shifts increase with "larger" average bond lengths. Such phenomenon was confirmed by molecular orbital calculations of s-electron density for tetrahderal ferric irons (Tang Kai, et al., 1980). As shown by the chemical analyses in Table 3, AEN2 is aluminum-free, whereas AEN1 and AEN3 contain significant amounts of aluminum which increase average bond length of the tetrahedral sites. This fact may explain why tetrahedral Fe^{3+} ions in AEN1 and AEN3 have slightly higher isomer shift values.

For a better correlation of ferric iron in tetrahedral coordination, Mossbauer parameters of aenigmatites were compared

with those of the structrally related sapphirine (Steffen & Seifert, in press; Bancroft, et al., 1968) Our results are consistent with their parameters for the second doublet (Table 7) of synthetic sapphirine having isomer shift (δ) and quadrupole splitting (Δ) values of 0.3 and 0.76 mm/sec, respectively. Their natural yellow sapphirine has δ of 0.3 mm/sec and Δ of 0.78 mm/sec. The assignment of Fe^{3+} ions to tetrahedral sites results in some aluminum being in octahedral coordination, which differs from conventional site occupancies deduced from chemical analyses. This will be discussed later.

Table 7. Mossbauer parameters of synthetic sapphirine* and natural yellow sapphirine**

	Synthetic sapphirine		natural sapphirine	
	doublet I	doublet II	doublet I	doublet II
δ	0.29	0.30	0.27	0.30
Δ	1.23	0.76	1.37	0.78
Width H	0.53	0.45	0.73	0.52
Width L	0.48	0.49	0.59	0.52
%Area	0.36	0.64	0.42	0.58

* from Steffen and Seifert, in press
** from Bancroft, et al., 1968
values in mm/sec relative to Fe foil
H and L refer to the high- and low-velocity components of the doublets, respectively
Both doublets are assigned to ferric in tetrahedral sites

It becomes apparent from the fitting procedures and derived Mossbauer parameters that no evidence was found for mixed valence iron cation species resulting from electron delocalization between Fe^{2+} and Fe^{3+}. If such phenomena exist in aenigmatite, an additional peak might be located on the inner limb of the high velocity envelope where it could correspond to the position of the present third peak. The matching peak for mixed valence species would be expected on the low velocity side of the low velocity envelope so as to give a smaller isomer shift than the normal value for discrete Fe^{2+} cations (usually lower than 1.00 mm/sec). However, that kind of fitting could not be achieved and the present fitting scheme indicated that the fitted line matched the spectrum envelope very well, especially in the limb areas of both high and low velocity regions. The author suggests that the aenigmatite specimens studied here do not show any evidence of $Fe^{2+} \rightarrow Fe^{3+}$ electron delocalization effects. The interpretation of peak areas and crystal chemistry of aenigmatite will be discussed in the next section.

2. Crystal Chemistry of Aenigmatites

Chemical data for the aenigmatites studied in this work are shown in Table 3 which summarizes wet chemical analyses for AEN1 and AEN2 and an electron microprobe analysis for AEN3. Because of the structural complexities, that is, the existence of several octahedral and tetrahedral sites and the possibility of different site occupancies by minor cations (Fe^{3+} and Al^{3+}), raw chemical data only cannot sufficiently describe the detailed crystal chemistry of aenigmatite. With the aid of additional information obtained from Mossbauer spectroscopy, more precise crystal chemistry can be deduced. In order to do so effectively, we shall now discuss how proportions of Fe^{2+} and Fe^{3+} can be determined from Mossbauer data and then compare the Fe^{3+}/Fe^{2+} ratios determined by the Mossbauer and wet chemical teniques.

In an electron microprobe analysis, total iron is usually expressed as weight percent of FeO. This means that ferric iron is calculated as the ferrous state which results in a lower weight percent of iron (expressed as FeO instead of Fe_2O_3) than the actual value. That is, total weight % of oxides determined by the microprobe will be lower than the sum obtained by wet analysis. Such discrepancies can be reduced by considering the percent of the actual Fe_2O_3 and multiplying the FeO content by the conversion factor 1.112 which is derived from the ratio of formula weights of $(^1/_2Fe_2O_3)/FeO$. The amount of iron present as ferric or ferrous can be determined directly

from the peak areas in the fitted Mossbauer spectra and can be expressed as an Fe^{3+}/Fe^{2+} ratio. Such ratio data for AEN1 and AEN2 in Table 8 indicate that Mossbauer analyses yield nearly the same results as found by wet analyses.

Using the electron microprobe data of AEN3, the correct weight percentages of FeO and Fe_2O_3 are determined as follows;

raw probe data: 41.13 wt. % FeO.

Mossbauer analysis suggests that

$Fe^{2+}/\Sigma\ Fe = 0.8794$ $Fe^{3+}/\Sigma\ Fe = 0.1206$.

Therefore, the amount of iron in the ferric state is

$41.13 \cdot 0.1206 = 4.960$ wt. %.

However, this value is not correct because this iron is considered as FeO, and it should be Fe_2O_3. The adjustment is made by multiplying by the factor 1.112:

$4.960 \cdot 1.112 = 5.516$ wt. % Fe_2O_3.

The value 5.52 is the actual weight percent Fe_2O_3 in AEN3. The corrected value of FeO is determined as the percentage of the probe data:

$41.13 \cdot 0.8794 = 36.17$ wt. % FeO.

The amounts of Fe^{3+} in tetrahedral sites and octahedral sites can be calculated directly from the area ratio of the two different ferric peaks. Table 8 gives the comparison between Mossbauer analyses and wet analyses.

Table 8. Ferric and ferrous chemical data of aenigmatite obtained from the Mossbauer peak areas and wet chemical analyses.

	AEN1		AEN2		AEN3
	Moss	Wet*	Moss	Wet*	Moss
wt. %					
Fe_2O_3	4.69	4.64	4.74	4.46	5.52
FeO	33.87	33.92	35.62	33.92	36.17
Fe^{3+}					
tet	0.56	0.52	0.558	0.213	0.636
oct	0.433	0.47	0.457	0.741	0.556
Fe^{2+}	8.065	8.066	8.473	8.537	8.698
Fe^{3+}/Fe^{2+}	0.12	0.12	0.12	0.11	0.14

* from Kelsey and McKie, 1964

Finally, the cation distribution among the structural sites of aenigmatite can be described completely by using the Mossbauer analyses for ferric and ferrous iron and the traditional crystal chemical approach.

In the assignment of tetrahedral sites, the discrepancy between Mossbauer analysis and traditional crystal chemical methods arises from the large amount of ferric iron in tetrahedral sites found by Mossbauer spectroscopy. According to Kelsey and McKie (1964), all available Si^{4+} and Al^{3+} occupy

the tetrahderal sites, leaving a small proportion of tetrahedral sites available to ferric iron. This results in Al^{3+} having a the relative enrichment over Fe^{3+} for the tetrahedral sites. However, the Mossbauer experiments indicates that a higher proportion of ferric iron occurs in tetrahedral coordination, resulting in an enrichment of Fe^{3+} over Al^{3+} for the tetrahedral sites. The values of Fe^{3+}/tet and Fe^{3+}/oct in Table 8 show the discrepancy between Mossbauer and wet analysis. The site occupancies yield 12 formula units of cations in tetrahedral coordination, based on the 40 anions (Cl^-, OH^-, O^{2-}) in the chemical formula.

The remainder of Al^{3+} and Fe^{3+} occupy octahedral sites together with Mg^{2+}, Ti^{4+}, and Fe^{2+}. Remaining deficiencies in the octahedral sites were filled by Mn^{2+}, Ca^{2+}, and even Zn^{2+} cations, yielding a total of 12 formula units of octahedral cations. Finally, large cations like Na^+, K^+, and the small amounts of Ca^{2+} fill the eight-fold coordination sites, amounting to 8 formula units. The complete cation distributions for the aenigmatite specimens are given in Table 9.

Cation distributions for AEN2 and AEN3 in Table 9 show that there is an excess of cations in tetrahedral sites and a deficiency in octahedral sites. This indicates that Mossbauer analysis overestimates the amount of ferric iron in tetrahedral sites. This experimental error may be due to the problem associated with fitting of low intensity ferric peaks which make

Table 9. Cation distributions in aenigmatite specimens

	AEN1	AEN2	AEN3
Si^{4+}	11.264	11.785	11.571
Al^{3+}	0.176		
Fe^{3+}	0.560	0.558	0.636
Σ 4	12.000	12.343	12.207
Al^{3+}	0.039		0.444
Fe^{3+}	0.433	0.457	0.556
Mg^{2+}	0.699	0.573	0.003
Ti^{4+}	2.066	1.777	1.626
Fe^{2+}	8.065	8.473	8.698
Mn^{2+}	0.593	0.429	0.202
Ca^{2+}	0.105		0.040
Zn^{2+}			0.036
Σ 6	12.000	11.709	11.605
Ca^{2+}	0.029		
Na^{+}	3.969	3.799	4.321
K^{+}	0.014	0.014	0.021
Σ 8	4.011	3.813	4.341
Cl^{-}	0.10		
OH^{-}	0.096		
O^{2-}	39.804	40.000	40.000
Σ	40.000	40.000	40.000

accurate fitting very difficult. If the excess amounts of tetrahedral Fe^{3+} are allocated to octahedral sites, the cation distributions are more reasonable. Even so, a deficiency still remained in octahedral sites of AEN3. This may be offset by appropriating some Na^{+} in higher coordination number sites to octahedral sites. However, such assignment of Na^{+} in octahedral coordination may be questionable.

IV. CONCLUSIONS

The Mossbauer study on three different aenigmatite specimens leads to the following conclusions:

1. Aenigmatite is a common consitituent of sodium-rich alkaline igneous rocks. Earlier uncertainties about its crystal chemistry and structure led to some confusion in name and identity which still exists. Through this study, two specimens from the Harvard collection (H85123 & H85123A) were found to be arfvedsonite and even in a recent paper (Steffer and Seifer, in press), amphibole was misinterpreted as aenigmatite.

2. Due to strong overlap in the low velocity region and small intensities of Fe^{3+} components, the fitting of aenigmatite Mossbauer spectra was heavily constrained and only successful in the spectra at room temperature. All spectra were fitted with nine peaks which consist of three doublets and a combined peak at low velocity (approximately 0.0 mm/sec) corresponding to two small independent peaks (approximately 0.6 and 1.0 mm/sec) in the high velocity region.

3. With isomer shifts between 1.10 and 1.18 mm/sec, three of the thedoublets are assigned to Fe^{2+} in octahedral coordination; Fe^{2+}(I) is attributed to M(3) + M(4) + M(6), Fe^{2+}(II) is

attributed to M(1) + M(2), and Fe^{2+}(III) is attributed to M(5), respectively. Their area ratio is approximately 3 : 2 : 1 which agrees with the multiplicity of sites for the three cation groups. Two ferric doublets are assigned to Fe^{3+} in tetrahedral coordination (δ = 0.28 - 0.33 mm/sec and Δ = 0.66 - 0.76 mm/sec) and Fe^{3+} in octahedral coordination (δ = 0.49 - 0.51 mm/sec and Δ = 1.07 mm/sec). Fe^{3+}/tet was also confirmed by comparison with structurally related sapphirine.

4. Using the peak areas for Fe^{2+} and Fe^{3+} peaks in the Mossbauer spectra, the electron microprobe data for iron were recalculated to give weight percentages of FeO and Fe_2O_3. Comparisons of Fe^{3+}/Fe^{2+} ratios determined wet chemically and by Mossbauer spectroscopy demonstrated the accuracy of Mossbauer analysis and yielded more precise crystal chemistry of aenigmatite than could be achieved by the traditional crystal chemical approach. The imbalance of total cation numbers in tetrahedral sites and octahedral sites indicates that some experimental error occurred due to overestimate of Fe^{3+}/tet. Such an error may be the result of difficulty in the resolution of very low intensity peaks. However, the existence of significant amounts of Fe^{3+}/tet suggests a different cation ordering in tetrahedral coordination from that deduced by traditional methods, that is, Fe^{3+} has a preference over Al^{3+} for the tetrahedral sites.

5. Finally, the spectra of aenigmatite specimens used in this study show no evidence of electron delocalization suggested by Burns (1981). However, this conclusion is not final because the three samples studied may not be representative of all aenigmatites. The author suggests that more specimens with higher Fe^{3+} ion concentration and further Mossbauer studies might yield evidence for electron delocalization in aenigmatites.

BIBLIOGRAPHY

Bancroft, G. M., 1973, Mossbauer Spectroscopy: Introduction to Inorganic Chemists and Geochemists, McGraw-Hill, N. Y.

Bancroft, G. M., R. G. Burns, and A. J. Stone, 1968, Applications of the Mossbauer effect to silicate mineralogy-II. Iron silicates of unknown and complex crystal structures, Geoch. et Cosmo. Acta, 32, 547 - 559.

Burns, R. G., 1981, Intervalence transitions in mixed-valence minerals of iron and titanium, Ann. Rev. Earth & Planet. Sci., 9, 345 - 383.

Cameron, K. L., M.F. Carman, and J. C. Butler, 1970, Rhönite from Big Bend National Park, Texas, Amer. Mineral., 55, 1587 - 1607.

Cannillo, E., F. Mazzi, J. H. Fang, P. D. Robinson, and Y. Ohya, 1971, The crystal structure of aenigmatite, Amer. Mineral., 56, 427 - 446.

Carmichael, I. S. E., 1962, Pantelleritic liquids and their phenocrysts, Min. Mag., 33, 86 -113.

Deer, W. A., R. A. Howie, and J. Zussman, 1978, Rock-Forming Minerals (2nd ed.): Vol. 2A, Single-Chain Silicates, John Wiley & Sons, N. Y.

Dollase, W. A., 1975, Statistical limitations of Mossbauer spectral fitting, Amer. Mineral., 60, 257 - 264.

Dornberger-Schiff, K. and S. Merlino, 1974, Order-disorder in sapphirine, aenigmatite and aenigmatite-like minerals, Acta Cryst., A30, 168 - 173.

Higgins, J.B., P. H. Ribbe, and R. K. Herd, 1979, Sapphirine I: Crystal chemical contributions, Contr. Min. Petr., 68, 349 -356.

Higgins, J. B. and P. H. Ribbe, 1979, Sapphirine II: A neutron and X-ray diffraction study of $(Mg-Al)^{VI}$ and $(Si-Al)^{IV}$ ordering in monoclinic sapphirine, Contr. Min. Petr., 68, 357 - 368.

Huggins, F. E., 1974, Mossbauer Studies of Iron Minerals Under Pressure of up to 200 Kilobars, Ph.D. Thesis, M.I.T., Cambridge, Massachusetts.

Kelsey, D. H. and D. McKie, 1964, The unit cell of aenigmatite, Min. Mag., 33, 986 - 1001.

Liebau, F., 1980, Classification of silicates, In P. H. Ribbe, ed., Orthosilicates, Rev. in Mineralogy Vol. 5, 1 - 24.

Machin, M. P. and P. Süsse, 1974, Serendibite: a new member of the aenigmatite structure group. Neues Jahrb. Min., Mh., 435 - 441.

McCammon, C. A. and R. G. Burns, 1979, The oxidation mechanism of vivianite as studied by Mossbauer spectroscopy, Amer. Mineral., 65, 361 -366.

Merlino, S., 1970, Crystal chemistry of aenigmatite, Chem. Comm., 20, 1288 - 1289.

Merlino, S., 1972, X-ray crystallography of krinovite, Z. Krist., 136, 81 -88.

Merlino, S., 1973, Polymorphism in sapphirine, Contr. Min. Petr., 41, 23 -29.

Merlino, S., 1980, Crystal structure of sapphirine - 1Tc, Zeit. fur Krist., 151, 91 -100.

Moore, P. B., 1969, The crystal structure of sapphirine, Amer. Mineral., 54, 34 - 49.

Morse, S. A. and J. H. Talley, 1971, Sapphirine reactions in deep-seated granulites near Wilson Lake, central Labrador, Canada, Earth Planet. Sci. Letters, 10, 325 - 328.

Nolet, D. A. and R. G. Burns, 1979, Ilvaite: a study of temperature dependent electron delocalizatrion by Mossbauer effect, Phy. Chem. Mineral., 4, 221 - 234.

Palache, C., 1933, Crystallographic notes on anapaite, aenigmatite, and endidymite, Z. Krist., 86, 280 - 291.

Ruby, S. L., 1973, Why MISFIT when you already have χ^2? In: Mossbauer Effect Methodology, Vol. 8 (J. Gruverman, ed.), Plenum Press, N. Y.

Steffen, G. and F. Seifert, 1982, Ferric iron in sapphirine: A Mossbauer spectroscopic study, in press.

Stone, A. J., H. J. Augard, and J. Fenger, 1969, General constrained non-linear regression for Mossbauer spectra. publ. Danish Atomic Energy Comm., R150-M-1348.

Tang Kai, A., H. Annersten, and T. Ericsson, 1980, Molecular orbital (MSX_α) calculations of s-electron densities of tetrahedrally coordinated ferric iron: Comparison with experimental isomer shifts, Phys. Chem. of Mineral., 5, 343 - 349.

Thompson, R. N. and J. E. Chisholm, 1969, Synthesis of aenigmatite, Min. Mag., 37, 820 - 829.

Yagi, K. and J. G. Souther, 1974, Aenigmatite from Mt. Edziza, British Columbia, Canada, Amer. Min., 59, 820 - 829.